

# Removal of styrene by the synthesized ZnO nanoparticles coated on the activated carbon adsorbent in the presence of UV irradiation

Mojtaba Nakhaei Pour<sup>1</sup>, Hossein Ali Rangkooy<sup>2,3</sup>, Fereshteh Jahani<sup>3</sup>, Ameneh Golbaghi<sup>3</sup>, Hosein Shojaee-Farah Abady<sup>4</sup>, Leila Nematpour<sup>3\*</sup>

<sup>1</sup>Occupational Health Engineering, Social Development and Health Promotion Research Center, Gonabad University of Medical Sciences, Gonabad, Iran

<sup>2</sup>Occupational Health Engineering, Environmental Technologies Research Center, Ahvaz Jundishapur University of Medical Sciences, Ahvaz, Iran

<sup>3</sup>Occupational Health Engineering, Department of Occupational Health, School of Health, Ahvaz Jundishapur University of Medical Sciences, Ahvaz, Iran

<sup>4</sup>Occupational Health Engineering, Department of Occupational Health Engineering, School of Health, Zabol University of Medical Sciences, Zabol, Iran

## Abstract

**Background:** Volatile organic compounds are the major environmental pollutants causing adverse effects on the human health and the environment, therefore, tremendous effort has been put toward eliminating these compounds.

**Methods:** In this study, the effect of synthesized nanoparticles on the removal of styrene from gas phase by photocatalytic process under UV irradiation in the cylindrical photoreactor was studied. The activated carbon-zinc oxide (AC-ZnO) catalysts were prepared at different weight ratios (6%, 12%, and 18%) of ZnO. The prepared catalyst was characterized using X-ray diffraction (XRD), field emission scanning electron microscopy (FESEM), and Brunauer-Emmett-Teller (BET) analyses. The effects of various parameters, such as concentrations of styrene, various weight percentage (wt%) of nanoparticles, and UV irradiation, were investigated. The efficiency of the AC-ZnO catalyst was determined based on its adsorption capacity, breakthrough time, and removal efficiency.

**Results:** It was revealed that the photocatalytic removal efficiency of styrene was high in the presence of both ZnO nanoparticle and AC under UV light. Under optimal conditions, the efficiency of UV/AC-ZnO 18%, UV/AC-ZnO 12%, and UV/AC-ZnO 6% catalysts was 77%, 86%, and 83%, respectively. By increasing the concentration of input styrene, the photocatalytic removal efficiency was reduced, while the adsorption capacity of styrene increased.

**Conclusion:** According to the results, the AC-ZnO 12% exhibited higher activity compared to other photocatalysts. Also, the amount of stabilized ZnO nanoparticles on the activated carbon affects the elimination rate of styrene.

**Keywords:** Photocatalysis, Activated carbon, Styrene, Zinc oxide

**Citation:** Nakhaei Pour M, Rangkooy HA, Jahani F, Golbaghi A, Shojaee-Farah Abady H, Nematpour L. Removal of styrene by the synthesized ZnO nanoparticles coated on the activated carbon adsorbent in the presence of UV irradiation. Environmental Health Engineering and Management Journal 2019; 6(4): 225–232. doi: 10.15171/EHEM.2019.25.

## Article History:

Received: 2 March 2019

Accepted: 16 July 2019

ePublished: 20 September 2019

## \*Correspondence to:

Leila Nematpour

Email: Lnematpour94@gmail.com

## Introduction

Volatile organic compounds (VOCs) are among the major pollutants released from various industrial processes (1). Styrene is a derivative of benzene and an important organic chemicals (2). Styrene is widely used in the production of plastics, rubber, resins, etc (3,4). Exposure to styrene can occur via inhalation or skin contact (5). Research has

shown that the highest exposures of human to styrene occurs in fiberglass and plastic manufacturing industries (5,6). Exposure to styrene can cause skin inflammation, eye and nose irritation, and breathing problems. The International Agency for Research on Cancer (IARC) has announced that styrene is possibly carcinogenic for human (7,8).



With the development of industry and the wide range of application of VOCs, researchers are looking for scientifically principled ways for removing these compounds. Nowadays, researchers have focused on the photocatalytic oxidation (PCO) technique in this regard (9). This technique is the most common method for removing VOCs, which commonly uses nano-semiconductor catalysts and ultraviolet (UV) light to convert organic compounds into harmless inorganic ones, such as  $\text{CO}_2$  and  $\text{H}_2\text{O}$  (10-12).

Among various semiconductors, titanium dioxide ( $\text{TiO}_2$ ) has been thoroughly investigated as an effective photocatalyst (13,14). However, zinc oxide (ZnO) can be considered as a very promising alternative since it is cost-effective and possesses a similar bandgap ( $\sim 3.3\text{eV}$ ) (15,16). Some studies have confirmed that ZnO exhibits a more efficient performance against  $\text{TiO}_2$  in the photodegradation of certain compounds in aqueous solutions, such as bleach pulp, phenylphenol, and phenol. Also, ZnO is abundant, not hazardous, and cost-effective (16,17).

Despite the positive attributes of these photocatalysts, poor adsorption of semiconductors (due to their small surface area) limits their application. To overcome this limitation, several attempts have been made to improve the efficiency of photocatalysts using suitable supports. In the last decade, nanoparticles and adsorbent surfaces as substrates have been simultaneously used for enhancing the removal efficiency of organic pollutants (18,19). In fact, by using suitable adsorbent surface areas and transmitting metal oxides next to one another, their adsorption capacity and ability of removing contaminants from the fluid flow can be simultaneously used (18).

Among various substrates, such as activated charcoal, zeolite, and cellulose, activated carbon has been widely used due to its high adsorption level, high porosity, non-polarity, low cost, and availability (20,21). Activated carbon has a large specific surface area ( $735.60\text{ m}^2\text{ g}^{-1}$ ) (22), and as a result, it is highly porous while having a high adsorption capacity and the ability to reactivate a material. For this reason, activated carbon is considered as a unique substrate (23,24). It seems that by using activated carbon adsorbents and transition metal oxides simultaneously, the adsorption capacities of activated carbon and the ability of metal oxide catalysts in removing contaminants from the fluid flow is enhanced (18).

This study aimed to assess the performance of the synthesized ZnO nanoparticles coated on the activated carbon (AC), in the removal of styrene from contaminated air streams. All the experiments were conducted at ambient temperature ( $\sim 26\pm 1^\circ\text{C}$ ). The experiments were set-up and run at Ahvaz chemical agents laboratory, Iran.

## Materials and Methods

### Chemicals

The activated carbon used in this study was obtained from

Merck Germany, with a particles diameter of 0.5-1 mm and a specific surface area of  $735.6\text{ m}^2\text{ g}^{-1}$ . Styrene with a purity over 99.98%, zinc nitrate 6 hydrate ( $\text{Zn}(\text{NO}_3)_2\cdot 6\text{H}_2\text{O}$ ), and hexadecyltrimethylammonium bromide (CTAB) were purchased from Merck Germany. Other necessary materials, such as hydrochloric acid and ethanol, were also obtained from Merck, Germany.

### Equipment

The prepared catalysts were characterized using X-ray diffraction (XRD), field emission scanning electron microscopy (FESEM), and Brunauer-Emmett-Teller (BET) test. The crystal phases of the prepared ZnO and AC-ZnO catalysts were analyzed using XRD (X-PERT PRO MPD instrument,  $\lambda = 1.5418\text{ \AA}$  and  $\theta = 4-80^\circ$ ) at room temperature. The specific surface area of ZnO, AC, and AC with different weight percentages of ZnO was determined using a Quantachrome ChemBET instrument (Micromeritics Instrument Corporation, TriStar II 3020 version 3.02, Serial # 1375 Unit 1 Port 1). The surface morphology of the samples was analyzed using FESEM technique (MIRA3 TESCAN-XMU, manufactured by TSCAN, America).

### ZnO nanoparticle synthesis

ZnO nanoparticles were synthesized via Sol-gel method. For this purpose, 5.76 g of zinc nitrate hexahydrate ( $\text{Zn}(\text{NO}_3)_2\cdot 6\text{H}_2\text{O}$ ) and 0.10 g of CTAB were firstly dissolved in 50 mL of deionized water in order to obtain solution A. Solution B was obtained by dissolving 1.31 g of sodium carbonate ( $\text{Na}_2\text{CO}_3$ ) in 50 mL of deionized water. Then, solution B was added dropwise to solution A under vigorous stirring. The stirring continued for 60 minutes to generate a white suspension. The produced precipitate was collected by centrifugation, filtered using a micrometer filter paper, and then, washed twice with deionized water and three times with ethanol. After washing, the precipitates were placed in an oven at  $100^\circ\text{C}$  overnight to be dried and later at  $300^\circ\text{C}$  for 2 hours to be calcined (25,26).

### Preparation of the AC-ZnO catalyst

The AC-ZnO catalyst was prepared in weight ratios of 6%, 12%, and 18% of ZnO. First, a certain amount of ZnO was weighed and poured into a flask to prepare a uniform suspension. The suspension was then placed in an ultrasonic device for 30 minutes. Next, a certain amount of the activated carbon was added to the suspension containing nanoparticles, and shaken continuously using a shaker for 12 hours until completely mixed and the ZnO nanoparticles were stabilized on the surface and in the pores of the activated carbon. Next, the mixture was passed through a paper filter and dried at  $100^\circ\text{C}$ , and in order to stabilize ZnO on the activated carbon and achieve calcination, the mixture was placed in an oven at  $300^\circ\text{C}$  for 2 hours.

### Experimental conditions

A dynamic photoreactor system was used to provide air containing styrene in desired concentrations. For the continuous system, the inlet air was pumped using a 51 W air pump at a pressure of 11.147 mm Hg (Hitachi Ltd, Japan) through a container filled with activated carbon and silica gel to remove any inlet air pollution. The air then entered into a humidification and concentration system. The system was operated at an initial styrene concentration of 20, 100, and 300 mg/L at a flow rate of 0.5 L/min (27). A cylindrical quartz glass reactor with a length, diameter, and thickness of 280, 20, and 2 mm, respectively, was used for full transfer of UV radiation. The inlet and outlet of the reactor were at a distance of 2 cm from both ends of the cylinder in opposite directions from each other. An 8-watt UVA lamp was located at the center of the cylinder and three 6-watt UVA lamps were located outside the cylinder. The AC-ZnO catalyst was placed within the reactor and around the inner lamp (Figure 1).

Next, the air flow containing styrene was passed through at a temperature of  $25 \pm 2^\circ\text{C}$ , humidity of 30%, flow rate of 0.5 L/min, and at concentrations of 20, 100, and 300 mg/L. The sampling section consisted of a sampling port at the outlet as well as the inlet of the reactor. Styrene concentration in the outlet stream was monitored online by a portable photoionization VOC detector (Phocheck Tiger, model 5000, Ion Science Ltd., UK, detection limit: 1 ppb – 10000 mg/L). The styrene was measured every 5 minutes throughout the experiment. In order to ensure the accuracy of the measured data for each sample, these concentrations were also measured using a gas chromatographer (Philips PU4410) equipped with a flame ionization detector. Removal efficiency was calculated by comparing the input concentration data ( $C_i$ ) and reactor

output ( $C_o$ ) using Eq. (1):

$$R = \frac{C_i - C_o}{C_i} \times 100 \quad (1)$$

### Results

#### Catalyst characteristics

Table 1 shows the surface area of the ZnO, AC, and AC-ZnO catalysts using BET. The surface area of the ZnO was  $12.86 \text{ m}^2/\text{g}$ , which is much lower than that of AC or AC-ZnO.

The XRD patterns of ZnO and AC-ZnO are presented in Figure 2. The XRD pattern of a pure substance is like the fingerprint of that substance. As shown in this figure, the main composed peak in the spectrum of ZnO belongs to Zn, and no peaks relating to impurities, such as hydroxide (OH), were detected, indicating that the synthesized nanoparticles are pure. Also, the XRD pattern of ZnO showed that ZnO is structurally stable and has a hexagonal wurtzite structure.

Figure 3 shows the FESEM images of AC, ZnO, and AC-

**Table 1.** Surface area of the catalysts

Parameter	ZnO	AC	AC-ZnO 6%	AC-ZnO 12%	AC-ZnO 18%
BET ( $\text{m}^2/\text{g}^{-1}$ )	12.86	735	697	685	668

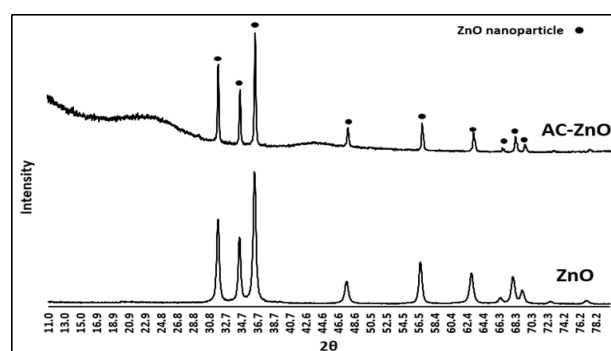


**Figure 2.** XRD pattern for ZnO and AC-ZnO.

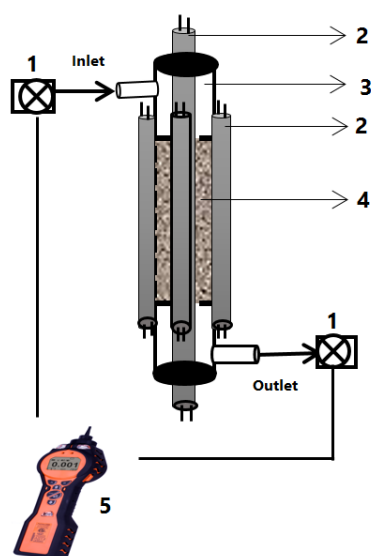


**Figure 1.** Schematic of the photoreactor and analyzer.

1) Sampling port, 2) UVA lamp, 3) Quartz glass cylinder, 4) Catalyst, 5) Analyzer (Phocheck Tiger)

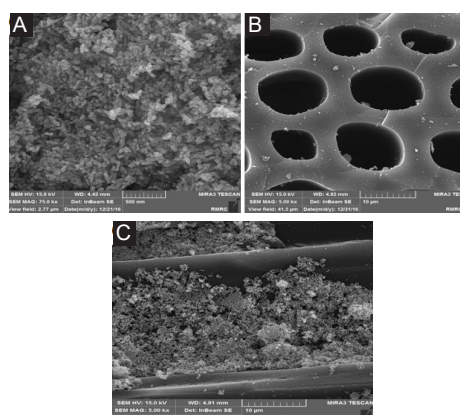


**Figure 3.** FESEM images of (a) Nano ZnO, (b) AC, and (c) AC-ZnO 12%.

ZnO. Based on these images, it can be concluded that the ZnO sample has a wide distribution of particle sizes ranging from 10 to 100 nm. Also, it was revealed that the nanoparticles have a spherical shape with irregular aggregations.

Elemental analysis of AC-ZnO 12% was performed using SEM-EDX. The results of this analysis are presented in Figure 4, indicating the presence of carbon, oxygen, and zinc elements in the sample, and also there was no impurities either.

**The loading effect of ZnO on the photocatalytic removal process**

Figures 5 and 6 show the photocatalytic removal efficiency of styrene and the effect of loading ZnO on the photocatalytic removal process at various concentrations of AC-ZnO 18%, AC-ZnO 12%, and AC-ZnO 6% catalysts. As can be seen, at concentration of 20 mg/L, when the percentage of ZnO nanoparticles increased from 6% to 12%, the removal efficiency of styrene increased from 77% to 86%. However, as the percentage of ZnO increased from 6% to 12%, the removal efficiency decreased to 83%. At concentrations of 100 and 300 mg/L, by increasing the wt% of the nanoparticles on the activated carbon from 6% to 12%, the removal efficiency increased, while by increasing the wt% of nano ZnO from 12% to 18%, the removal efficiency reduced.

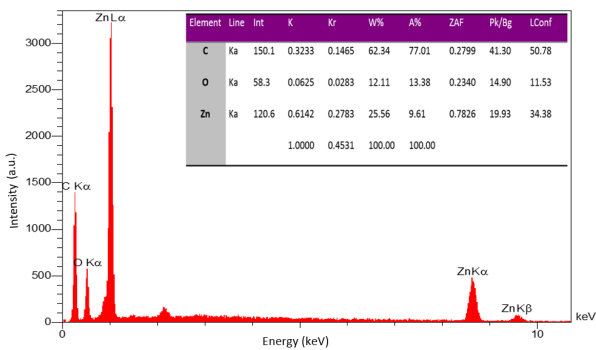


Figure 4. EDX analysis of AC-ZnO 12%.

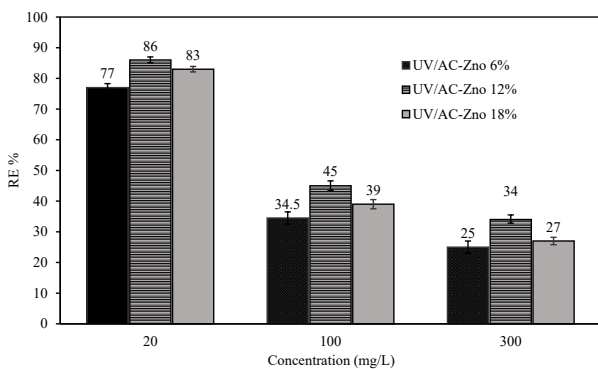


Figure 5. Styrene removal efficiency at different concentrations.

**The effect of UV irradiation**

Figure 7 shows the effect of UV irradiation on the removal of styrene. The results showed that the stabilization of ZnO nanoparticles on the activated carbon reduced the styrene adsorption. So that styrene appeared in AC and AC-ZnO beds at time of 43.5 and 42 hours, respectively. Also, AC and AC-ZnO beds were saturated after 78 and 76 hours, respectively. The results also showed that the adsorption of styrene by the activated carbon in the presence and absence of UV irradiation was the same. But in the reactor containing AC-ZnO, when UV was on, styrene vapors were removed by photocatalytic activity of ZnO nanoparticles, and styrene appeared after 45.5 hours. Also after 75 hours, the removal efficiency of styrene was 85.75%.

**The effect of styrene concentration on photocatalytic removal**

Figure 8 shows the effect of styrene concentration on the photocatalytic removal efficiency of AC-ZnO 12%. By increasing the concentration of input styrene, the photocatalytic removal efficiency reduced. By increasing the input concentration from 20 to 300 mg/L, the removal efficiency reduced from 86% to 34%.

**Adsorption capacity**

To determine the adsorption capacity up to the

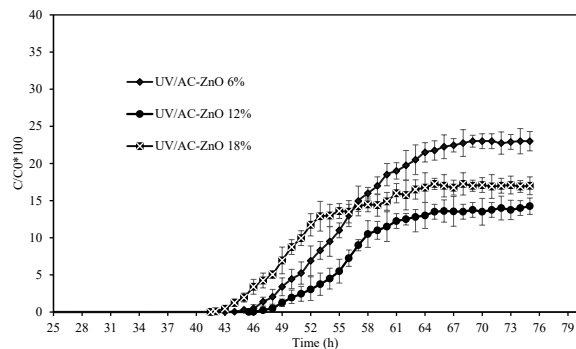


Figure 6. Photocatalytic removal of styrene using AC-ZnO 6%, 12%, 18% at concentration of 20 mg/L.

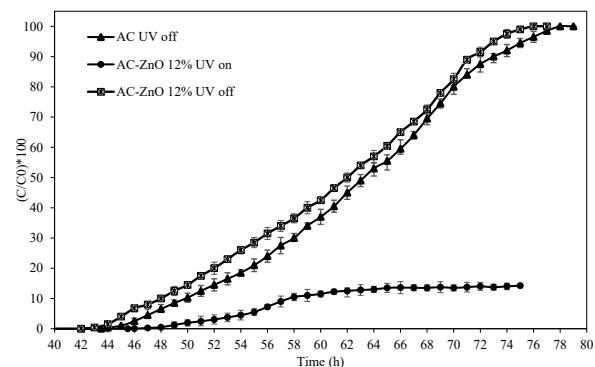
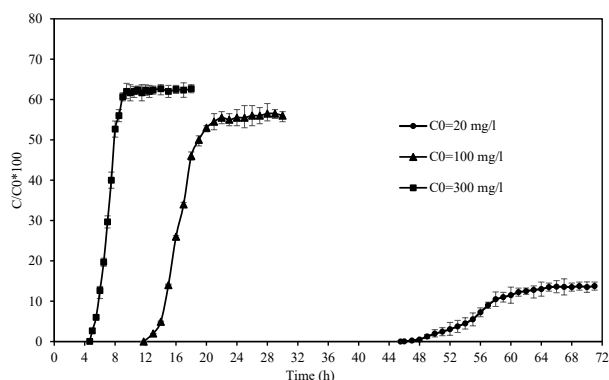


Figure 7. Effect of UV irradiation (C0= 20 mg/L)..



**Figure 8.** The effects of concentration on the photocatalytic removal of styrene by the process of UV/AC-ZnO 12%.

breakthrough point, the following equation was used:

$$BC = \frac{Q.C.Tbk}{M_{adsorbent}} \quad (2)$$

where  $BC$  is the mass of styrene adsorbed by the substrate ( $\text{mg/g}^{-1}$ ),  $Q$  is the inflow discharge of the reactor ( $\text{m}^3/\text{h}$ ),  $C$  is styrene concentration ( $\text{mg/g}^{-3}$ ), and  $Tbk$  is the breakthrough time (h).

The calculated adsorption capacity for AC-ZnO catalyst with different percentages of 6%, 12%, and 18% are presented in Table 2.

### Discussion

The results show that by increasing the amount of ZnO, the surface area of AC-ZnO decreases. In general, specific surface area a catalyst is the main factor influencing the catalyst activity (4). A wide surface area is just one of the factors contributing to the high efficiency of adsorbing pollutants, but the destruction of organic pollutants by ZnO compensates for the limited surface area, and subsequently, achieves a higher efficiency compared to the AC substrate. Pulido Melián et al showed that ZnO particles cause a reduction in the specific surface area of the activated carbon in the AC-ZnO catalyst (28).

The peaks of the XRD pattern for the AC-ZnO catalyst indicated successful stabilization of the nanoparticles on the activated carbon. Although carbon is heavier than the AC-ZnO catalyst, but its peak characteristic was not

observed. This could be due to the absence of a crystalline structure within carbon.

Texture and morphology of the catalysts are very important parameters that affect photocatalytic activity. FESEM images clearly showed that ZnO nanoparticles were coated on the activated carbon. Also, the images are indicators of uniform coating of photocatalyst ZnO nanoparticles on the activated carbon.

A possible explanation for reduced removal efficiency could be that by increasing ZnO nanoparticles on the activated carbon, the pores and cavities of the activated carbon (bands or agents of adsorption) get blocked, which leads to a reduction in the adsorption of styrene and a lower rate of contact between styrene and ZnO, and as a result, reduces styrene removal efficiency. The results indicated that AC-ZnO 12% in the presence of UV irradiation more effectively removed styrene because styrene adsorbed by AC in the composite AC-ZnO could then be continuously decomposed by UV in the presence of the ZnO photocatalyst on the composite. Using AC, the removal of styrene from air occurs only by adsorption, as it does not have any photoactivity. On UV/AC-ZnO catalysts, both processes, adsorption of styrene by the activated carbon and its degradation by ZnO photocatalysts, occur at the same time. Since the adsorption process of the activated carbon proceeds much faster than the degradation by photocatalysis, the removal of styrene occurs mainly by the former rather than the later. The removal of styrene gradually increases as a result of the combination of both processes, i.e. adsorption and degradation. Therefore, in addition to the synergistic effect of ZnO loading, the findings of the present study suggest that the rate of stabilized ZnO nanoparticles on the activated carbon is effective in the photocatalytic removal. Studies have suggested that the increase of the percentage of catalyst to a certain extent could be due to an increase in the contaminant removal (29).

Various amounts of nanoparticles on the adsorbent have been reported in the literature as the optimal amounts (30-32). In a study by Kuo et al on the removal of toluene using AC- $\text{TiO}_2$  with different wt% of nanoparticles, it was observed that AC- $\text{TiO}_2$  catalyst with a  $\text{TiO}_2$  wt% of 13%, had the highest amount of contaminant removal,

**Table 2.** Calculated adsorption capacities and breakthrough of UV/AC-ZnO

Catalyst	Concentration (mg/L)	Flow Rate ( $\text{L}/\text{min}^{-1}$ )	Breakthrough (h)	Adsorption Capacity ( $\text{mg}/\text{g}^{-1}$ )
AC-ZnO 6%	20	0.5	54	68.906
	100		13:40	87.198
	300		5:15	100.490
AC-ZnO 12%	20	0.5	52:30	66.992
	100		13:20	85.072
	300		5:10	98.882
AC-ZnO 18%	20	0.5	48:10	61.463
	100		11:15	71.779
	300		3:50	73.374

but by increasing the percentage of  $\text{TiO}_2$  to 16.7% or 20%, pollutant removal capacity decreased (30). Another study by Chen and Tang on the removal of trichloroethylene from the air using  $\text{ZnO}/\text{Al}_2\text{O}_3$  catalysts showed that the optimal amount of the activated metal on the catalyst was 5% (31). In the other study, the optimal amount of  $\text{TiO}_2$  photocatalyst on the activated carbon adsorbent was reported to be 13% (32). In the present study, the optimal amount of fixed ZnO on the activated carbon among the three weight percentages (6%, 12%, and 18%) was 12%, which was 86% efficient at a concentration of 20 mg/L. In the photocatalytic removal process, gas molecules must first be adsorbed onto the catalytic active sites, and then, be destroyed. Therefore, as far as these sites are not saturated with increasing concentrations, removal efficiency increases. However, after saturation, removal rate does not change significantly (33). Also, at high concentrations, electrons and more reactive compounds, such as OH, are required for the degradation of pollutants (13,30). Other studies also found that by increasing concentration, removal efficiency decreases. Rangkooy et al reported that by increasing the initial concentration of formaldehyde from 2.5 to 25  $\text{mg}/\text{m}^3$ , the photocatalytic removal efficiency of ZnO-99BC and ZnO-95BC catalysts decreased from 53% to 26.4% and from 73% to 40%, respectively (34).

Based on Table 2, it can be concluded that in all catalysts, increasing the concentration of styrene leads to a decrease in the breakthrough time and an increase in the adsorption capacity. Gangupomu et al also reported that by reducing the concentration of the input pollutant, breakthrough times increases while adsorption capacity decreases (35). Studies have shown that by increasing concentration, a larger mass of pollutant per unit of time is removed from the air flow, and as a result, breakthrough time and saturation of the adsorbent reduce (36,37). On the other hand, the ratio of the increase of pollutant molecules to the number of active sites on the catalyst surface raises. By increasing the penetration into the pores of the catalyst and the speed of propagation, adsorption occurs faster. This means that full saturation of the active sites on the surface of the adsorbent occurs in a shorter time. However, the removal efficiency of Zn 12% photocatalyst was higher than the other photocatalysts. Thus, it can be concluded that the adsorption capacity was not the sole cause of the high efficiency observed for the catalyst.

Studies have shown that increasing concentration causes removal of a larger mass of styrene from the air per unit of time. Therefore, the breakpoint of the column and saturated adsorber is reduced (32,36). On the other hand, by increasing the concentration of styrene, the ratio of the number of styrene molecules to the number of active sites on the catalyst surface increases and due to the increase in the speed of propagation and penetration into the pores of the catalyst, adsorption would occur faster. As a result, complete saturation of the adsorption sites on the catalyst

surface occurs within a shorter time (38). The results of this study showed that increasing input concentration leads to the faster saturation of the absorbent and hastens the breakthrough point, which is consistent with the results of other studies (39-41).

### Conclusion

In this study, ZnO nanoparticles were synthesized successfully by the sol-gel method and a series of AC-ZnO photocatalysts prepared with various ZnO percentage ratios. Also, the characterization of the ZnO coated AC with a Zn weight ratio of 12% showed that the ZnO nanoparticles attached properly to the adsorbent surface. Coating ZnO on AC decreases its surface area and AC-ZnO with more ZnO ratio had a less surface area. Among various AC-ZnO catalysts, the highest removal efficiency of styrene was achieved using AC-ZnO 12% while the 6% variant had the highest adsorption capacity. A synergistic effect was also observed when ZnO and AC were simultaneously used for the photocatalytic degradation of styrene.

### Acknowledgements

This work was supported by Ahvaz Jundishapur University of Medical Sciences (Grant No: 95s86). The authors wish to thank Ahvaz Jundishapur University of Medical Sciences for its financial support.

### Ethical issues

The author hereby certify that all data collected during the research are as expressed in the manuscript, and no data from the study has been or will be published elsewhere separately.

### Competing interests

The authors have declared that they have no conflicts of interests.

### Authors' contribution

All authors contributed in data collection, analysis, and interpretation. All authors reviewed, refined, and approved the manuscript.

### References

1. Khan FI, Ghoshal AK. Removal of volatile organic compounds from polluted air. *J Loss Prev Process Ind* 2000; 13(6): 527-45. doi: 10.1016/S0950-4230(00)00007-3.
2. Lim M, Rudolph V, Anpo M, Lu GQ. Fluidized-bed photocatalytic degradation of airborne styrene. *Catal Today* 2008; 131(1): 548-52. doi: 10.1016/j.cattod.2007.10.092.
3. Jorio H, Bibeau L, Heitz M. Biofiltration of air contaminated by styrene: effect of nitrogen supply, gas flow rate, and inlet concentration. *Environ Sci Technol* 2000; 34(9): 1764-71. doi: 10.1021/es990911c.
4. Rangkooy HA, Nakhaei M, Jahani F, Salari S, Nematpour L, Fouladi B. Effect of nano- $\text{TiO}_2$  immobilized on activated carbon, zeolite Y and ZSM-5 on the removal of styrene

- vapours from polluted air. *J Nanostruct* 2018; 8(3): 307-15. doi: 10.22052/jns.2018.03.011.
5. Rueff J, Teixeira JP, Santos LS, Gaspar JF. Genetic effects and biotoxicity monitoring of occupational styrene exposure. *Clin Chim Acta* 2009; 399(1-2): 8-23. doi: 10.1016/j.cca.2008.09.012.
  6. Rangkooy HA, Nakhaei Pour M, Fouladi Dehaghi B. Efficiency evaluation of the photocatalytic degradation of zinc oxide nanoparticles immobilized on modified zeolites in the removal of styrene vapor from air. *Korean J Chem Eng* 2017; 34(12): 3142-9. doi: 10.1007/s11814-017-0174-2.
  7. Vodicka P, Koskinen M, Arand M, Oesch F, Hemminki K. Spectrum of styrene-induced DNA adducts: the relationship to other biomarkers and prospects in human biomonitoring. *Mutat Res* 2002; 511(3): 239-54. doi: 10.1016/s1383-5742(02)00012-1.
  8. Tamime AY. *Microbial Toxins in Dairy Products*. USA: John Wiley & Sons; 2017.
  9. de Luna MD, Lin JC, Gotostos MJ, Lu MC. Photocatalytic oxidation of acetaminophen using carbon self-doped titanium dioxide. *Sustain Environ Res* 2016; 26(4): 161-7. doi: 10.1016/j.serj.2016.02.001.
  10. Mohamed RM, McKinney DL, Sigmund WM. Enhanced nanocatalysts. *Materials Science and Engineering: R: Reports* 2012; 73(1): 1-13. doi: 10.1016/j.mser.2011.09.001.
  11. Al-Nour GY. Photocatalytic degradation of organic contaminants in the presence of graphite-supported and unsupported ZnO modified with CdS particles [dissertation]. Nablus: An-Najah National University; 2009.
  12. Thiruvenkatachari R, Vigneswaran S, Moon IS. A review on UV/TiO<sub>2</sub> photocatalytic oxidation process (Journal Review). *Korean J Chem Eng* 2008; 25(1): 64-72. doi: 10.1007/s11814-008-0011-8.
  13. Hashimoto K, Irie H, Fujishima A. TiO<sub>2</sub> photocatalysis: a historical overview and future prospects. *Jpn J Appl Phys* 2005; 44(12R): 8269-85. doi: 10.1143/jjap.44.8269.
  14. Fujishima A, Zhang X, Tryk DA. TiO<sub>2</sub> photocatalysis and related surface phenomena. *Surf Sci Rep* 2008; 63(12): 515-82. doi: 10.1016/j.surfrep.2008.10.001.
  15. Muruganandham M, Zhang Y, Suri R, Lee GJ, Chen PK, Hsieh SH, et al. Environmental applications of ZnO materials. *J Nanosci Nanotechnol* 2015; 15(9): 6900-13. doi: 10.1166/jnn.2015.10725.
  16. Khodja AA, Sehili T, Pilichowski JF, Boule P. Photocatalytic degradation of 2-phenylphenol on TiO<sub>2</sub> and ZnO in aqueous suspensions. *J Photochem Photobiol A Chem* 2001; 141(2-3): 231-9. doi: 10.1016/S1010-6030(01)00423-3.
  17. Lizama C, Freer J, Baeza J, Mansilla HD. Optimized photodegradation of Reactive Blue 19 on TiO<sub>2</sub> and ZnO suspensions. *Catal Today* 2002; 76(2-4): 235-46. doi: 10.1016/S0920-5861(02)00222-5.
  18. Deng QF, Ren TZ, Yuan ZY. Mesoporous manganese oxide nanoparticles for the catalytic total oxidation of toluene. *Reaction Kinetics, Mechanisms and Catalysis* 2013; 108(2): 507-18. doi: 10.1007/s11144-012-0528-z.
  19. Pelaez M, Nolan NT, Pillai SC, Seery MK, Falaras P, Kontos AG, et al. A review on the visible light active titanium dioxide photocatalysts for environmental applications. *Appl Catal B Environ* 2012; 125: 331-49. doi: 10.1016/j.apcatb.2012.05.036.
  20. Qu F, Zhu L, Yang K. Adsorption behaviors of volatile organic compounds (VOCs) on porous clay heterostructures (PCH). *J Hazard Mater* 2009; 170(1): 7-12. doi: 10.1016/j.jhazmat.2009.05.027.
  21. Gil RR, Ruiz B, Lozano MS, Martín MJ, Fuente E. VOCs removal by adsorption onto activated carbons from biocollagenic wastes of vegetable tanning. *Chem Eng J* 2014; 245: 80-8. doi: 10.1016/j.cej.2014.02.012.
  22. Kermani M, Pourmoghaddas H, Bina B, Khazaei Z. Removal of phenol from aqueous solutions by rice husk ash and activated carbon. *Pak J Biol Sci* 2006; 9(10): 1905-10. doi: 10.3923/pjbs.2006.1905.1910.
  23. Matos J, Laine J, Herrmann JM. Effect of the type of activated carbons on the photocatalytic degradation of aqueous organic pollutants by UV-irradiated titania. *J Catal* 2001; 200(1): 10-20. doi: 10.1006/jcat.2001.3191.
  24. Araña J, Doña Rodríguez JM, Tello Rendón E, Garriga i Cabo C, González Díaz O, Herrera-Melián JA, et al. TiO<sub>2</sub> activation by using activated carbon as a support: Part I. surface characterisation and decantability study. *Appl Catal B Environ* 2003; 44(2): 161-72. doi: 10.1016/S0926-3373(03)00107-3.
  25. Yu C, Yang K, Shu Q, Yu JC, Cao F, Li X. Preparation of WO<sub>3</sub>/ZnO composite photocatalyst and its photocatalytic performance. *Chin J Catal* 2011; 32(3-4): 555-65. doi: 10.1016/S1872-2067(10)60212-4.
  26. Akin B, Oner M. Aqueous pathways for formation of zinc oxide particles in the presence of carboxymethyl inulin. *Res Chem Intermediat* 2012; 38(7): 1511-25. doi: 10.1007/s11164-011-0481-x.
  27. Asilian H, Khavanin A, Afzali M, Dehestani S, Soleimanion A. Removal of styrene from air by natural and modified zeolite. *Health Scope* 2012; 1(1): 7-11. doi: 10.5812/jhs.4592.
  28. Pulido Melián E, González Díaz O, Doña Rodríguez JM, Colón G, Araña J, Herrera Melián J, et al. ZnO activation by using activated carbon as a support: characterisation and photoreactivity. *Applied Catalysis A: General* 2009; 364(1-2): 174-81. doi: 10.1016/j.apcata.2009.05.042.
  29. Lu Y, Wang D, Ma C, Yang H. The effect of activated carbon adsorption on the photocatalytic removal of formaldehyde. *Build Environ* 2010; 45(3): 615-21. doi: 10.1016/j.buildenv.2009.07.019.
  30. Kuo HP, Wu CT, Hsu RC. Continuous reduction of toluene vapours from the contaminated gas stream in a fluidised bed photoreactor. *Powder Technol* 2009; 195(1): 50-6. doi: 10.1016/j.powtec.2009.05.010.
  31. Chen JC, Tang CT. Preparation and application of granular ZnO/Al<sub>2</sub>O<sub>3</sub> catalyst for the removal of hazardous trichloroethylene. *J Hazard Mater* 2007; 142(1-2): 88-96. doi: 10.1016/j.jhazmat.2006.07.061.
  32. Mo J, Zhang Y, Xu Q, Lamson JJ, Zhao R. Photocatalytic purification of volatile organic compounds in indoor air: a literature review. *Atmos Environ* 2009; 43(14): 2229-46. doi: 10.1016/j.atmosenv.2009.01.034.
  33. Jo WK, Kim JT. Application of visible-light photocatalysis with nitrogen-doped or unmodified titanium dioxide for control of indoor-level volatile organic compounds. *J Hazard Mater* 2009; 164(1): 360-6. doi: 10.1016/j.jhazmat.2008.08.033.
  34. Rangkooy HA, Rezaei A, Khavanin A, Joneidi A. Removal of Formaldehyde from Air Using Modified Bone Char. *Jundishapur Scientific Medical Journal* 2013; 12(2): 197-

208. [In Persian].
35. Gangupomu RH, Sattler ML, Ramirez D. Comparative study of carbon nanotubes and granular activated carbon: physicochemical properties and adsorption capacities. *J Hazard Mater* 2016; 302: 362-74. doi: 10.1016/j.jhazmat.2015.09.002.
36. Mishra T, Mohapatra P, Parida KM. Synthesis, characterisation and catalytic evaluation of iron–manganese mixed oxide pillared clay for VOC decomposition reaction. *Appl Catal B Environ* 2008; 79(3): 279-85. doi: 10.1016/j.apcatb.2007.10.030.
37. Wang HC, Liang HS, Chang MB. Chlorobenzene oxidation using ozone over iron oxide and manganese oxide catalysts. *J Hazard Mater* 2011; 186(2-3): 1781-7. doi: 10.1016/j.jhazmat.2010.12.070.
38. Rezaei E, Soltan J, Chen N. Catalytic oxidation of toluene by ozone over alumina supported manganese oxides: effect of catalyst loading. *Appl Catal B Environ* 2013; 136-137: 239-47. doi: 10.1016/j.apcatb.2013.01.061.
39. Baral SS, Das N, Ramulu TS, Sahoo SK, Das SN, Chaudhury GR. Removal of Cr (VI) by thermally activated weed *Salvinia cucullata* in a fixed-bed column. *J Hazard Mater* 2009; 161(2-3): 1427-35. doi: 10.1016/j.jhazmat.2008.04.127.
40. Malkoc E, Nuhoglu Y, Dundar M. Adsorption of chromium (VI) on pomace--an olive oil industry waste: batch and column studies. *J Hazard Mater* 2006; 138(1): 142-51. doi: 10.1016/j.jhazmat.2006.05.051.
41. Rao KS, Anand S, Venkateswarlu P. Modeling the kinetics of Cd (II) adsorption on *Syzygium cumini* L leaf powder in a fixed bed mini column. *J Ind Eng Chem* 2011; 17(2): 174-81. doi: 10.1016/j.jiec.2011.02.003.